

# The quest for neutrinoless double beta decay: Pseudo-Dirac, Majorana and sterile neutrinos

A. Meroni,<sup>1,2</sup> E. Peinado,<sup>2</sup>

<sup>1</sup>*Dipartimento di Matematica e Fisica, Università di Roma Tre,  
Via della Vasca Navale 84, I-00146 Rome, Italy*

<sup>2</sup>*INFN, Laboratori Nazionali di Frascati, Via Enrico Fermi 40, I-00044 Frascati, Italy*  
(Dated: December 6, 2024)

In this paper we analyze the neutrinoless double beta decay predictions in some scenarios with admixture of pseudo-Dirac and Majorana neutrinos in the 3 and 3+1 neutrino frameworks. We found that some of the cases can be falsifiable in near-term and future generations of neutrinoless double beta decay experiments even for the normal neutrino mass hierarchy. In the 3+1 framework we consider the sterile neutrino with a mass of the order of 1 eV. The complementarity between cosmological constraints and the future sensitivity for the next generations of the neutrinoless double beta decay searches is exploited.

## I. INTRODUCTION

The observation of neutrino oscillations [1–4] implies that neutrinos are massive particles. The fact that the neutrino masses scale is several orders of magnitude smaller than the rest of the fermions of the Standard Model (SM)<sup>1</sup>, suggest an extension in which neutrinos are generally expected to be of Majorana type, violating the total lepton number symmetry, such as for example the so-called seesaw mechanism [8–12] which account for the observed smallness of neutrino mass relative to that of charged fermions.

The only feasible underground experiments at present that could be able to pin down the Majorana nature of massive neutrinos, namely to prove the electron neutrino Majorana effective mass  $|m_{\beta\beta}|$ , and thus giving information on the violation of the total lepton number symmetry [13] are those searching for neutrinoless double beta  $((\beta\beta)_{0\nu})$ -decay [14]:  $(A, Z) \rightarrow (A, Z+2) + e^- + e^-$ .

Despite intense ongoing efforts, the decay has not been observed yet, but important progresses have been made and especially the data from

the GERDA-I [15] have shown that the claim by Klapdor-Kleingrothaus *et. al.* [16] is now strongly disfavored (see [17, 18] for experimental review). On the other hand  $|\Delta L| = 2$  processes can be tested in colliders, which opens the possibility to investigate all the elements of the neutrino mass matrix,  $M_{\alpha\beta}^\nu$  with  $\alpha, \beta = e, \mu, \tau$  (for details see [19]).

In summary the status of lepton and baryon number symmetries remains one of the most interesting unsolved question in particle physics [20], and neutrinos could very well be Dirac fermions.

## II. NEUTRINOLESS DOUBLE BETA DECAY: GENERAL FRAMEWORK

In the  $3\nu$  mixing scheme with massive neutrinos,  $\chi_j$ , being Majorana particles, the  $(\beta\beta)_{0\nu}$ -decay can be generated only by the  $(V - A)$  charged current weak interaction via the exchange of the three Majorana neutrinos  $\chi_j$  having masses  $m_j \lesssim$  a few eV. The amplitude of the decay is proportional to the so-called Majorana effective mass [21–23]:

$$|m_{\beta\beta}| = \left| m_1 |U_{e1}|^2 + m_2 |U_{e2}|^2 e^{i\lambda_{21}} + m_3 |U_{e3}|^2 e^{i\lambda_{31}} \right|. \quad (1)$$

In eq. (1),  $U_{ej}$ ,  $j = 1, 2, 3$ , are the elements of the first row of the Pontecorvo-Maki-Nakagawa-Sakata (PMNS) matrix,  $U$ , describing the neutrino mixing [24], and  $\lambda_{21}$  and  $\lambda_{31}$  are the two Majorana CP violation (CPV) phases. In the standard parametrization of the neutrino

mixing matrix, we have that the elements,  $U_{ej}$ , depend only on the reactor and the solar neutrino mixing angles,  $\theta_{13}$  and  $\theta_{12}$ . More precisely these elements can be written as:

$$\begin{aligned} |U_{e1}| &= \cos \theta_{12} \cos \theta_{13}, \\ |U_{e2}| &= \sin \theta_{12} \cos \theta_{13}, \\ |U_{e3}| &= \sin \theta_{13}. \end{aligned}$$

Neutrino oscillation data are still compatible with two type of neutrino mass spectra: i) normal ordered,  $m_1 < m_2 < m_3$  and ii) inverted ordered,

<sup>1</sup> The most recent cosmological upper bound for the sum of neutrino masses is  $\sum m_\nu \leq (0.2 - 0.6) \text{eV}$  [5], this will be complemented by the future sensitivity from the Katrin experiment [6, 7].

$m_3 < m_1 < m_2$ . The ordering of the masses determines a peculiar dependence of  $|m_{\beta\beta}|$  with respect to the lightest neutrino mass and therefore also with respect to the sum of the light active neutrinos  $\sum_i m_i$ . Depending on the value of the lightest neutrino mass,  $\min(m_j)$ , and on the hierarchy of the neutrino masses, the value of  $|m_{\beta\beta}|$  can be:

- *quasi-degenerate (QD)*:  
 $m_1 \approx m_2 \approx m_3 \approx m_0 \gtrsim 0.1\text{eV}$  gives  
 $|m_{\beta\beta}| \gtrsim 0.05\text{eV}$ .
- *inverted hierarchical (IH)*:  
 $m_3 \ll m_1 < m_2$  so  $m_{1,2} \sim \sqrt{\Delta m_A^2}$  gives  
 $0.015 \lesssim |m_{\beta\beta}| \lesssim 0.05\text{eV}$ .
- *normal hierarchical (NH)*:  
 $m_1 \ll m_2 < m_3$  so  $m_2 \sim \sqrt{\Delta m_\odot^2}$ ,  $m_3 \sim \sqrt{\Delta m_A^2}$  and so  $|m_{\beta\beta}| \lesssim 0.015\text{eV}$ .

Further, the minimum for the sum of the neutrino masses compatible with current neutrino oscillation data, namely when the lightest neutrino is massless, is  $(\sum_i m_i)_{\min} = 5.87 \times 10^{-2} \text{ eV}$  for NH and  $(\sum_i m_i)_{\min} = 9.78 \times 10^{-2} \text{ eV}$  for IH.

The  $(\beta\beta)_{0\nu}$ -decay experimental search is therefore compelling due to the enormous impact in determining the nature of massive neutrinos, in constraining the absolute neutrino mass scale as well as in the possibility to test the type of hierarchy for the neutrino masses. So far, current experiments did not observe the decay. From those searches, one can derive lower bounds on the half-lives of the utilized isotopes (see e.g. [18] for a summary). Combining the results by GERDA-I, the Heidelberg-Moscow and IGEX data sets, a limit on the  $^{76}\text{Ge}$  half-life was obtained  $T_{1/2}^{0\nu}(^{76}\text{Ge}) > 3.0 \times 10^{25} \text{ yr}$  at 90% C.L. [15]. Limits for  $T_{1/2}^{0\nu}(^{136}\text{Xe})$  has been set by the EXO-200 and KamLAND-ZEN Collaborations [25, 26].

The next generation of  $(\beta\beta)_{0\nu}$ -decay experiments ( $\gtrsim 5\text{yr}$ ), such as GERDA-II ( $^{76}\text{Ge}$ ), SuperNEMO ( $^{82}\text{Se}$ ) CUORE ( $^{130}\text{Te}$ ) and nEXO-200 ( $^{136}\text{Xe}$ ) to name a few, have been planned to reach a sensitivity of  $T_{1/2}^{0\nu} \sim (1 - 1.5) \times 10^{26} \text{ yr}$ . This is meant to explore the inverted hierarchical region for  $|m_{\beta\beta}|$ , see the dashed region in Fig. (2). Since  $|m_{\beta\beta}|$  scales like  $\sqrt{T_{1/2}^{0\nu}}$  one can expect to push down  $|m_{\beta\beta}|$  of a factor of 3 or 4 with respect to the present lower bounds. Of course this could be not enough to cover the entire IH region, so at the moment many efforts are focused to reach values for  $|m_{\beta\beta}|$  around 10 meV. In this case detector technology plays a crucial role (a

reasonable signal-to-background ratio in the energy interval  $\Delta E$  of approximately a full width at half maximum (FWHM) around the Q-value is indeed related to possible high resolution detectors) together with the choice of the isotope used in the experiment.

Even though for the current running and near-term  $(\beta\beta)_{0\nu}$ -decay experiments will probably be difficult to explore the entire IH region it makes sense, from a theoretical point of view, to consider potential  $(\beta\beta)_{0\nu}$ -decay experiments aiming to measure half-lives of the order of  $10^{27}$  yrs or more. These generation of experiments, that we will labelled in the following as *mega*-experiments for  $T_{1/2}^{0\nu} \sim 10^{27}$  yrs and *ultimate*-experiments for  $T_{1/2}^{0\nu} \sim 10^{29}$  yrs [27], could test several scenarios involving Majorana neutrinos.

The  $(\beta\beta)_{0\nu}$ -decay experimental searches are also complementary to  $\beta$ -decay and cosmology, which has now entered its precision era [28, 29]. The constraints given by the Planck Collaboration on the sum of the light active neutrinos which were obtained from the measurements of the cosmic microwave background (CMB) temperature and lensing-potential power spectra make tantalizing these kind of combined analysis. We will consider as reference value the limit [5]

$$\sum_i m_i \leq 0.23\text{eV} \quad 95\% \text{ C.L.} \quad (2)$$

Future large scale structure surveys like the recent approved EUCLID [30], will allow to constrain  $\sum_i m_i$  up to few meV if is combined with the Planck data. We will consider in the following a future sensitivity of  $\sum_i m_i \lesssim 15 \text{ meV}$ .

The complementarity of  $|m_{\beta\beta}|$  and the constraints from cosmological observables is starting to be relevant in scenarios or models for neutrino physics<sup>2</sup>. More over, the limits from cosmology for the neutrino masses will be complemented by the the Tritium-beta decay experiment KATRIN [6, 7] whose sensitivity for the neutrino mass is expected to be around 0.2 eV.

In this work we explore testable scenarios in view of the next *mega*- and *ultimate*-generation of  $(\beta\beta)_{0\nu}$ -decay searches such as the admixture of pseudo-Dirac and Majorana neutrinos. Along the line with previous works (see e.g. [35]) we explore how the standard predictions for  $(\beta\beta)_{0\nu}$ -decay are considerably modified with the most recent neutrino oscillation data [36–38] and especially we investigate which of these scenarios

<sup>2</sup> See for instance the case of zero textures [31] and neutrino mass sum rules [32–34].

can be experimentally reachable in the *mega*- and *ultimate*-generations even for the NH spectrum (in the standard case in fact strong cancellations could occur leading to a zero  $|m_{\beta\beta}|$ ). Further, it is also known that in the presence of extra light sterile neutrinos, with square mass difference of the order of  $1 \text{ eV}^2$ , the  $|m_{\beta\beta}|$  is also modified [39, 40]. We will show how the analysis for  $(\beta\beta)_{0\nu}$ -decay and pseudo-Dirac neutrinos changes in the presence of one extra sterile state.

### III. LIGHT PSEUDO-DIRAC NEUTRINOS

As it is well known in the three Majorana neutrino framework the  $(\beta\beta)_{0\nu}$ -decay amplitude can well be zero in the NH case due to internal cancellations operated by the two Majorana phases spanning values in the range  $[0, 2\pi]$ . This behavior is not present in the IH case [41]. Further, in the NH scheme, uncertainties in the parameters governing neutrino oscillations, namely the angles and the two square mass differences, determine the existence of a quite large interval for the absolute neutrino mass scale in which  $|m_{\beta\beta}|$  can be zero. In the case in which at least one of the light active neutrinos  $\chi_i$ ,  $i = 1, 2, 3$  is a Dirac fermion, such field (which is the field with definite mass eigenstate) does not participate in the amplitude of the  $(\beta\beta)_{0\nu}$ -decay since it is distinct from its antiparticle and thus it is not possible to Wick-contract the neutrino field operator in order to obtain a neutrino propagator [13].

In this framework neutrinos are usually referred as pseudo-Dirac particles —when the two neutrinos are active-sterile we have the so-called quasi-Dirac neutrino [13] and when they are active-active we have the so called pseudo-Dirac neutrino [42]<sup>3</sup>. In this scenario the prediction for the  $(\beta\beta)_{0\nu}$ -decay half-life and thus for  $|m_{\beta\beta}|$  can deeply be modified.

In Fig. (1) and (2) we show the dependence of  $|m_{\beta\beta}|$  with respect to the sum of the light active states  $\sum_i m_i$  in the case of NH and IH respectively if only one of the neutrinos  $\chi_i$  is a Dirac fermion. In both plots we show the dashed contour which corresponds to the general allowed  $3\sigma$  region in the standard 3 Majorana neutrino case. The light (Yellow) region corresponds to a  $3\sigma$  uncertainty in the oscillation parameters while the dark (Gray) area indicates the prediction for  $|m_{\beta\beta}|$  for the best fit values in ref. [38]. In the NH case it is clear from the plots that if  $\chi_1$  is a Dirac parti-

cle then a lower limit for  $|m_{\beta\beta}|$  is found (differently from [35] the current value for  $\theta_{13}$  determine a non vanishing  $|m_{\beta\beta}|$ ). If instead  $\chi_2$  (or  $\chi_3$ ) are Dirac then a cancellation is still possible especially for  $\sum_i m_i$  quite near the lower limit given by the current oscillation experiments. The vertical solid line on those plots represents the Planck+WP+BAO limit given in eq. (2) while the vertical dashed line delimiting the shaded area is indicating the sensitivity of the next-generation of cosmological surveys i.e.  $\sum_i m_i \lesssim 15 \text{ meV}$ . The three horizontal bands indicate the GERDA-I limit and the two ranges for  $|m_{\beta\beta}|$  corresponding to the *mega*- and *ultimate*- $(\beta\beta)_{0\nu}$ -decay experiments (the intervals for  $|m_{\beta\beta}|$  has been computed using the NMEs used in [45]). For the IH scenario in Fig. (2) there is no complete cancelation for the  $|m_{\beta\beta}|$  (as in the usual three Majorana neutrino case), so all these scenario can be falsified in the next generation of  $(\beta\beta)_{0\nu}$ -decay experiments.

The case when two of the active states are Dirac particles are represented in the plots in Fig. (3) for NH and in Fig. (4) for IH. Here again the light (Yellow) region corresponds to a  $3\sigma$  uncertainty in the oscillation parameters while the thick solid line is determined with the best fit values in ref. [38]. The NH cases can all be tested in the *mega*-generation (in the case  $\chi_2$  and  $\chi_3$  are both Dirac then the interval of  $|m_{\beta\beta}| \sim 0$  corresponds to the limit of a massless neutrino). In the case of IH if  $(\chi_1, \chi_3)$  or  $(\chi_2, \chi_3)$  are Dirac fermions then they can be also tested by the *mega*-generation while the case of  $(\chi_1, \chi_2)$  will be very difficult if not impossible to rule out.

### IV. EXTRA STERILE NEUTRINOS

In the last decade the framework of 3-neutrino mixing has been challenged by the existence of experimental anomalies found in the i) results of the LSND [46] and MiniBooNE experiments [47] ii) re-analyses of the short baseline (SBL) reactor neutrino oscillation data using newly calculated fluxes of reactor  $\bar{\nu}_e$ , which detect a “disappearance” of the reactor  $\bar{\nu}_e$  (“reactor neutrino anomaly”) [48, 49] iii) results of the calibration experiments of the radio-chemical Gallium solar neutrino detectors GALLEX and SAGE (“Gallium anomaly”)[50, 51] —for a review see e.g. [52]. These anomalies could be explained enlarging the field content in the neutrino sector with one or more massive neutrinos with a square mass difference around  $1 \text{ eV}^2$ .

<sup>3</sup> For examples of models see for instance [35, 43, 44].

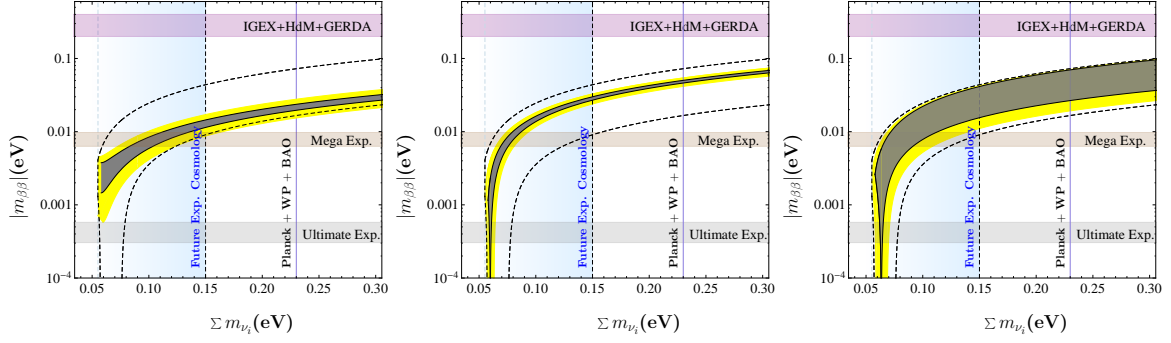


Figure 1. Plots for  $|m_{\beta\beta}|$  vs  $\sum_i m_i$  for the NH case in the case in which respectively, from the left to the right,  $\chi_1$  or  $\chi_2$  or  $\chi_3$  is a Dirac fermion and therefore the related contribution is not present in  $(\beta\beta)_{0\nu}$ -decay amplitude. The light (Yellow) region corresponds to a  $3\sigma$  uncertainty in the oscillation parameters while the dark (Gray) area indicates the prediction for  $|m_{\beta\beta}|$  for the best fit values given in [38]. The solid vertical line corresponds to the Planck constraint in eq. (2). The shaded area for  $\sum_i m_i \lesssim 15$  meV indicate the future cosmological sensitivity. The dashed contour indicate the standard predictions with three Majorana active neutrinos.

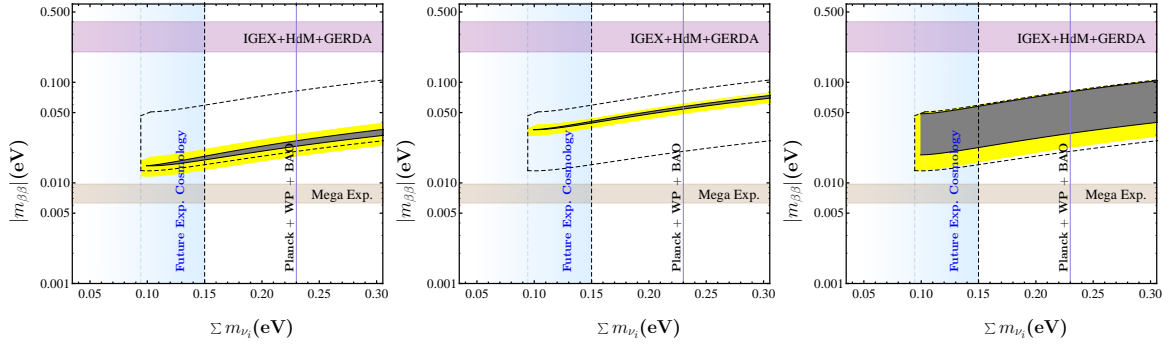


Figure 2. Plots for  $|m_{\beta\beta}|$  vs  $\sum_i m_i$  for the IH case in the case in which respectively, from the left to the right,  $\chi_1$  or  $\chi_2$  or  $\chi_3$  is a Dirac fermion. The dashed contour indicate the standard predictions with three Majorana active neutrinos. The same colors of Fig. (1) are used for the allowed regions.

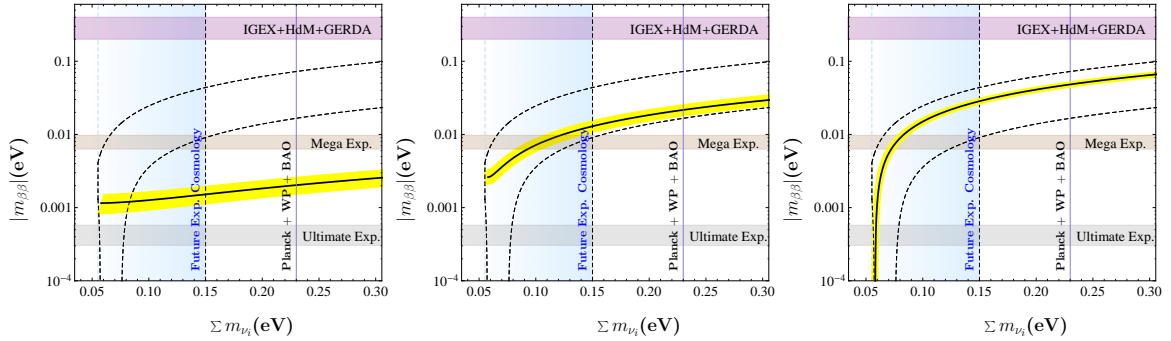


Figure 3. Plots for  $|m_{\beta\beta}|$  vs  $\sum_i m_i$  for the NH case in the case in which respectively, from the left to the right,  $(\chi_1, \chi_2)$  or  $(\chi_1, \chi_3)$  or  $(\chi_2, \chi_3)$  are Dirac fermions. The same colors of Fig. (1) are used for the allowed regions.

It is worth stressing that if this extra sterile state exists it would be completely thermalised in the early universe through mixing and scattering processes. However this is not confirmed by recent cosmological results which actually seem to disfavour these scenarios since such sterile state(s) would lead to a too strong suppression of structure

formation. Nevertheless sterile states with 1 eV mass, as indicated by SBL data, are still possible if either some neutrino-antineutrino asymmetry is at work in order to inhibit the sterile neutrino production in the early universe or a modification of the cosmological model is provided. In any case a mechanism preventing a full thermalization is needed (see [53] and references therein). It has been noticed in some works (see e.g. [39, 40]) that

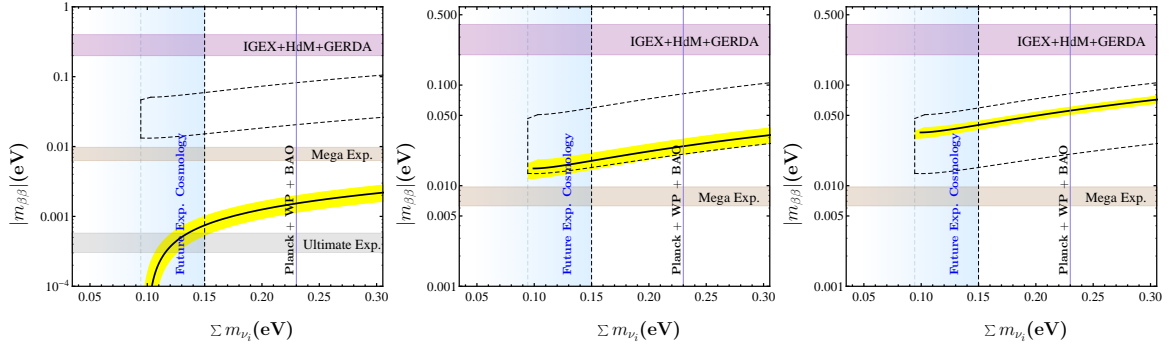


Figure 4. Plots for  $|m_{\beta\beta}|$  vs  $\sum_i m_i$  for the IH case in the case in which respectively, from the left to the right,  $(\chi_1, \chi_2)$  or  $(\chi_1, \chi_3)$  or  $(\chi_2, \chi_3)$  are Dirac fermions. The same colors of Fig. (1) are used for the allowed regions.

if one or two sterile Majorana neutrinos exist than they deeply modify the predictions for the  $(\beta\beta)_{0\nu}$ -decay. In the simplest scheme with one extra sterile neutrino, the so called 3 + 1 scheme, the matrix which describes neutrino mixing is now a  $4 \times 4$  unitary matrix which can be written as:

$$U = O_{34}V_{24}O_{23}O_{14}V_{13}V_{12} \times \text{diag}(1, e^{i\lambda_1}, e^{i\lambda_2}, e^{i\lambda_3}), \quad (3)$$

where  $O_{ij}$  and  $V_{kl}$  are real and complex rotations in  $i - j$  and  $k - l$  planes respectively, while  $\lambda_1, \lambda_2$  and  $\lambda_3$  are three CPV Majorana phases. In the effective Majorana mass  $|m_{\beta\beta}|$  only the elements

of the first row of the neutrino mixing matrix are relevant and their expressions can be written in a completely generic way as:

$$\begin{aligned} U_{e1} &= c_{12}c_{13}c_{14}, & U_{e2} &= e^{i\alpha/2}c_{13}c_{14}s_{12}, \\ U_{e3} &= e^{i\beta/2}c_{14}s_{13}, & U_{e4} &= e^{i\gamma/2}s_{14}, \end{aligned} \quad (4)$$

where we have used the standard notation  $c_{ij} \equiv \cos \theta_{ij}$  and  $s_{ij} \equiv \sin \theta_{ij}$  and  $\alpha, \beta$  and  $\gamma$  are a definite combination of the phases appearing in  $U$ . The element  $U_{e4}$ , and thus the angle  $\theta_{14}$ , describes the coupling of fourth neutrino  $\chi_4$  to the electron in the weak charged lepton current. The  $|m_{\beta\beta}|$  in this framework has the form:

$$|m_{\beta\beta}| = \left| m_1 |U_{e1}|^2 + m_2 |U_{e2}|^2 e^{i\alpha} + m_3 |U_{e3}|^2 e^{i\beta} + m_4 |U_{e4}|^2 e^{i\gamma} \right|. \quad (5)$$

Depending on the neutrino mass hierarchy, we will have:

- NH:

$$\begin{aligned} m_1 &\equiv m, & m_2 &= \sqrt{m^2 + \Delta m_{21}^2}, \\ m_3 &= \sqrt{m^2 + \Delta m_{21}^2 + \Delta m_{31}^2}, & m_4 &= \sqrt{m^2 + \Delta m_{41}^2} \end{aligned}$$

- IH:

$$\begin{aligned} m_1 &\equiv \sqrt{m^2 + \Delta m_{31}^2}, & m_2 &= \sqrt{m^2 + \Delta m_{21}^2 + \Delta m_{31}^2}, \\ m_3 &= m, & m_4 &= \sqrt{m^2 + \Delta m_{41}^2} \end{aligned}$$

In this section we want to illustrate the predictions for  $|m_{\beta\beta}|$  in the scenario with one extra Majorana sterile state,  $\chi_4$ , and three light active states  $\chi_1, \chi_2, \chi_3$  which can be pseudo-Dirac or Majorana particles. We will consider as reference value for  $\sin \theta_{14}$  and  $\Delta m_{41}^2$  the result obtained in

the global analyses performed in [54]<sup>4</sup>:

<sup>4</sup> For another global fit see [55]. Here we only give an example of how the  $|m_{\beta\beta}|$  is modified in the scenario of pseudo-Dirac neutrinos and one Majorana sterile state.

$$\sin \theta_{14} = 0.15, \quad \Delta m_{41}^2 = 0.93 \text{ eV}^2 \quad (6)$$

In Fig. (5) we show the  $|m_{\beta\beta}|$  versus the lightest neutrino mass  $m_\nu^{\text{light}}$  in the standard  $3\nu$  framework. In this case for both NH and IH the  $|m_{\beta\beta}|$  can vanish. Moreover for small absolute masses, namely for  $m_\nu^{\text{light}} < 0.01 \text{ eV}$  and  $|m_{\beta\beta}| < 0.01 \text{ eV}$  only IH is possible therefore only the *mega*- and *ultimate*-generation of  $(\beta\beta)_{0\nu}$ -decay experiments might constrain this scenario.

As in the previous section we analyze first of all the cases in which one of the lightest states  $\chi_1$ ,  $\chi_2$  or  $\chi_3$  is a Dirac neutrino. The results are shown in Fig. (6) and Fig. (7) for NH and IH respectively. In both plots we consider a  $3\sigma$  uncertainty in the oscillation parameters which corresponds to the light shaded region while the color

shaded area determines the allowed range for the best fit values of ref. [38]. As it is clear from the plots strong cancellations could be at work in  $|m_{\beta\beta}|$  for most of the cases both in the NH and in IH. In the NH case the intervals for the lightest mass where a complete cancellation occurs are in the region  $m_\nu^{\text{light}} \equiv m_1 > 0.01 \text{ eV}$ . In the IH scheme instead the cancellation can be realized for smaller, or even zero,  $m_\nu^{\text{light}} \equiv m_3$ . There is only one case, e.g. when  $\chi_2$  is the Dirac particle, where for any value of  $m_3$   $|m_{\beta\beta}| \gtrsim 5 \text{ meV}$ . In this case  $|m_{\beta\beta}|$  has a similar behaviour with respect to the standard IH three neutrino case.

More interestingly if a couple of the lightest states are Dirac fermions than of course in some cases the relative cancellations among the different terms are less effective so in the NH with Dirac ( $\chi_1, \chi_2$ ) and in IH in the cases with ( $\chi_1, \chi_2$ ) and ( $\chi_2, \chi_3$ )  $|m_{\beta\beta}|$  could well be test in the next generation of experiments like GERDA-II, CUORE, etc. This is depicted in Fig. (8) and (9).

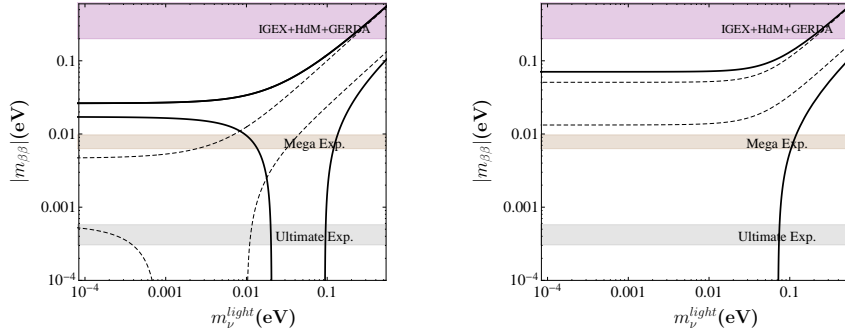


Figure 5. Plots for  $|m_{\beta\beta}|$  vs  $m_\nu^{\text{light}}$  in the scenario with 1 extra sterile state with  $\Delta m_{SBL}^2 = 0.93 \text{ eV}^2$  and  $\sin \theta_{14} = 0.15$  for NH (left panel) and IH (right panel). The dotted contours define the allowed range for  $|m_{\beta\beta}|$  in the  $3\nu$  framework. See text for further details.

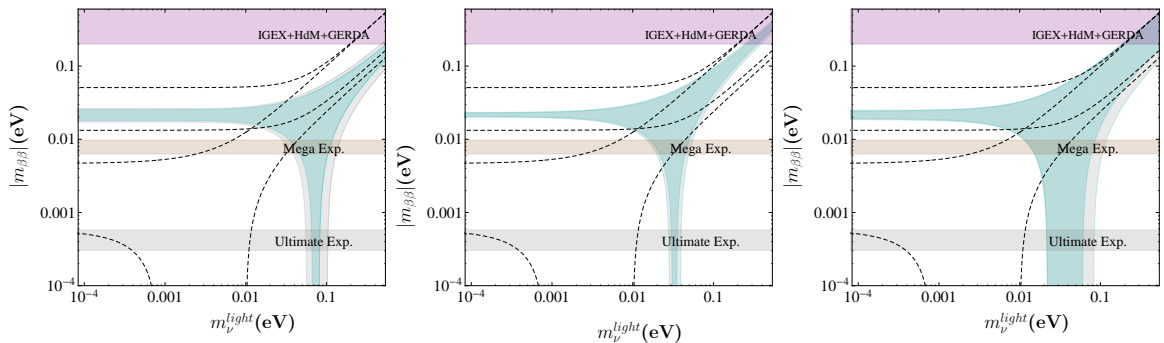


Figure 6. Plots for  $|m_{\beta\beta}|$  vs  $m_\nu^{\text{light}}$  for the NH case in the presence of one extra sterile neutrino in the case in which respectively, from the left to the right,  $\chi_1$  or  $\chi_2$  or  $\chi_3$  are Dirac fermions. The light (Gray) shaded area is the  $3\sigma$  allowed range given by oscillation data while the darker (Blue) shaded area is obtained from the best fit values in [38]. The dashed contour corresponds to the predictions for the  $3\nu$  case.

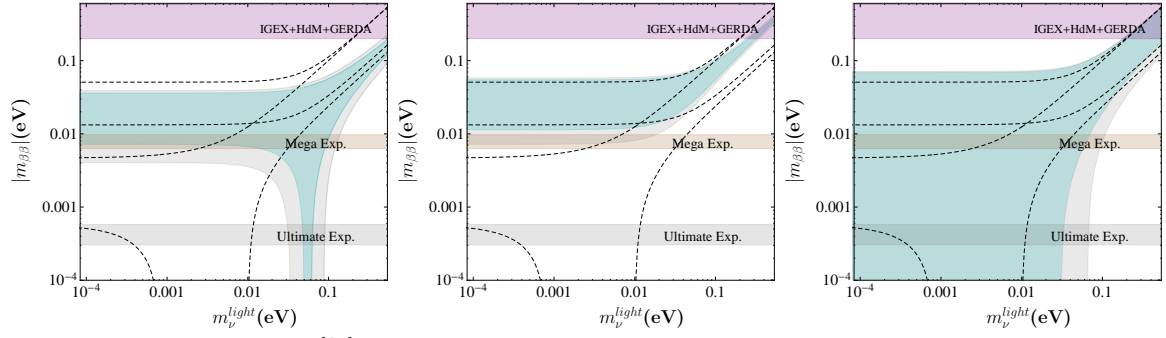


Figure 7. Plots for  $|m_{\beta\beta}|$  vs  $m_{\nu}^{light}$  for the IH case in the presence of one extra sterile neutrino in the case in which respectively, from the left to the right,  $\chi_1$  or  $\chi_2$  or  $\chi_3$  are Dirac fermions. The light and darker shaded areas are given as in Fig. 6.

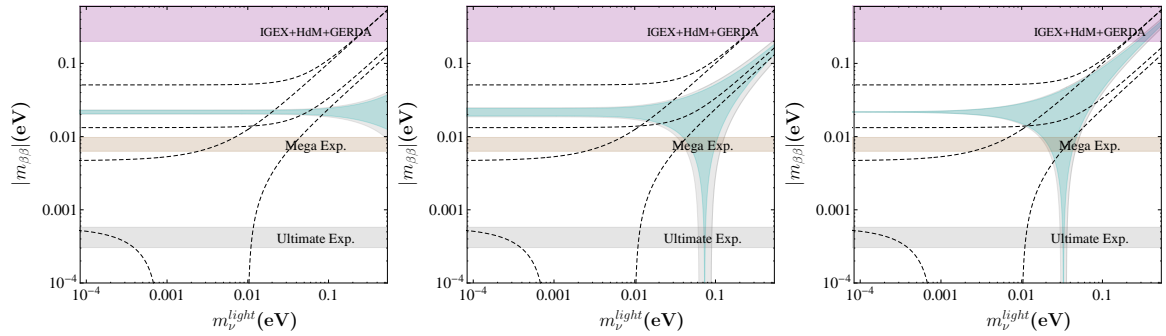


Figure 8. Plots for  $|m_{\beta\beta}|$  vs  $m_{\nu}^{light}$  for the NH case in the presence of one extra sterile neutrino state and in the case in which respectively, from the left to the right,  $(\chi_1, \chi_2)$  or  $(\chi_1, \chi_3)$  or  $(\chi_2, \chi_3)$  are Dirac fermions. The light and darker shaded areas are given as in Fig. 6.

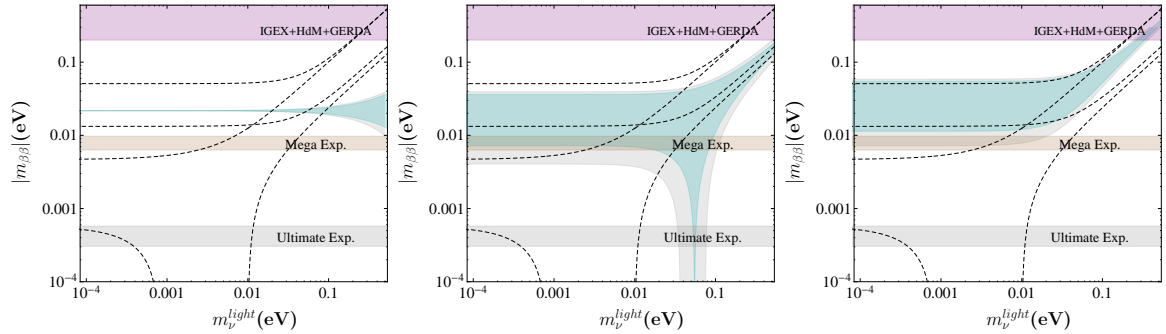


Figure 9. Plots for  $|m_{\beta\beta}|$  vs  $m_{\nu}^{light}$  for the IH case in the presence of one extra sterile neutrino state and in the case in which respectively, from the left to the right,  $(\chi_1, \chi_2)$  or  $(\chi_1, \chi_3)$  or  $(\chi_2, \chi_3)$  are Dirac fermions. The light and darker shaded areas are given as in Fig. 6.

## V. DISCUSSION

The current and near term neutrinoless double beta decay  $((\beta\beta)_{0\nu}$ -decay) experiments will be able to explore the region for  $|m_{\beta\beta}| \gtrsim 0.01$  eV. Hopefully with experiments such as GERDA-II, CUORE, nEXO etc. most of this region will be investigated but if the decay is not observed new experimental efforts will be required. From the theoretical point of view, it is also necessary to

understand which phenomenological frameworks could be tested in the next generation of  $(\beta\beta)_{0\nu}$ -decay experiments and also with the future *mega*- and *ultimate*-generations. In particular, It makes sense to investigate which scenarios for the NH spectrum can be experimentally reachable in the *mega*- and *ultimate*-generations, since in the standard three Majorana neutrino framework a complete cancellation can occur.

In this work we have analyzed the case in which

one or two active neutrinos are Dirac particles for both NH and IH. We found that due to narrow  $3\sigma$  range for  $\theta_{13}$  most of the cases we analyzed with one Dirac neutrino, could be falsifiable in the  $(\beta\beta)_{0\nu}$ -decay *mega*-generation since a complete cancellation not always occurs. In fact for the NH case there is no cancellation when the neutrino  $\chi_1$  is Dirac, see the plot on the left of Fig. (1). On the opposite, if a complete cancellation is realized, this occurs in a region where the lightest state is almost massless, see the plot in the center and on the right of Fig. (1). In the case of two Dirac neutrinos, a cancellation occurs only when the Dirac neutrinos are  $(\chi_2, \chi_3)$ , see the plot in the right side of Fig. (3).

In the second part of the work we have analyzed the allowed region for  $(\beta\beta)_{0\nu}$ -decay in the presence of pseudo-Dirac neutrinos together with an extra sterile neutrino state with mass of the order of 1 eV, as hinted by a number of anomalies arising in short baseline neutrino oscillation experiments. In this case if one of the active state is Dirac then in all the cases we analyzed but one, strong cancellations can occur. However, it is notable that for NH, these scenarios are considerably different from the standard three-neutrino case because the interval for the lightest neutrino mass in which the  $|m_{\beta\beta}|$  is zero is different. If instead two of the active states are Dirac fermions then the situation is more favorable and some cases are in the range of the next generation experiments. In summary, it

make sense from a theoretical perspective to analyze different scenarios for the nature of massive neutrinos that could be tested through terrestrial experiments. This means not only neutrinos as pure Dirac or pure Majorana particles but also the possibility that both natures coexist, even if from the theoretical point of view is less appealing.

## VI. ACKNOWLEDGMENTS

The authors fully acknowledge interesting correspondence with R. Brugnera, S. Pastor and E. Giusarma. A.M. acknowledge MIUR (Italy) for financial support under the program “Futuro in Ricerca 2010”, (RBFR10O36O).

## VII. APPENDIX

In this appendix for completeness we show the  $|m_{\beta\beta}|$  versus the sum of the three light active states in the case one extra sterile neutrino is added, see Fig. 10. We show as well  $|m_{\beta\beta}|$  vs the sum of the active neutrinos in the pseudo-Dirac scenarios considered in Section IV. In Figs. 11, 12, 13 and 14 the light shaded regions correspond to the  $3\sigma$  uncertainty in the oscillation parameters while the darker shaded area determines the allowed range for the best fit values of ref. [38].

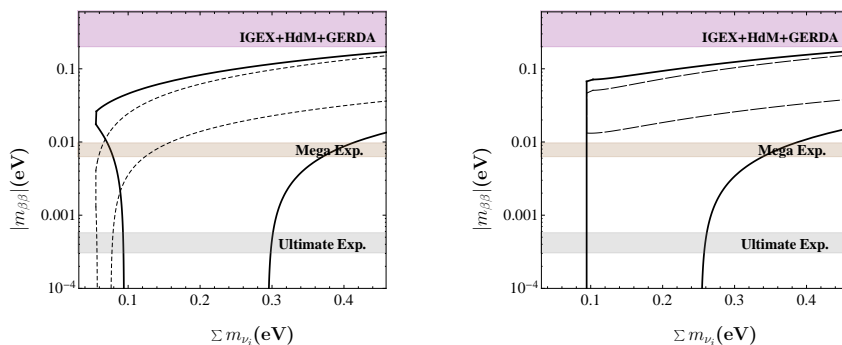


Figure 10. Plots for  $|m_{\beta\beta}|$  vs  $\sum_i m_i$  in the 3+1 scenario i.e. with 1 extra sterile state with  $\Delta m_{SBL}^2 = 0.93 eV^2$  and  $\sin \theta_{14} = 0.15$  for NH (left panel) and IH (right panel). The dotted contours define the allowed range for  $|m_{\beta\beta}|$  in the  $3\nu$  framework.



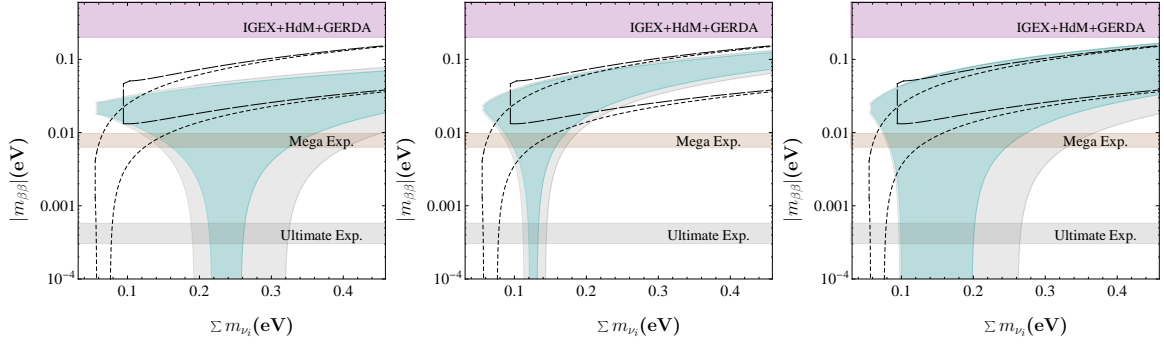


Figure 11. Plots for  $|m_{\beta\beta}|$  vs  $\sum_i m_i$  in the 3+1 scenario for the NH case in the case in which respectively, from the left to the right,  $\chi_1$  or  $\chi_2$  or  $\chi_3$  are Dirac fermions. The light (Gray) shaded area is the  $3\sigma$  allowed range given by oscillation data while the darker (Blue) shaded area is obtained from the best fit values in [38]. The short (long) dashed contours correspond to the predictions for the  $3\nu$  case.

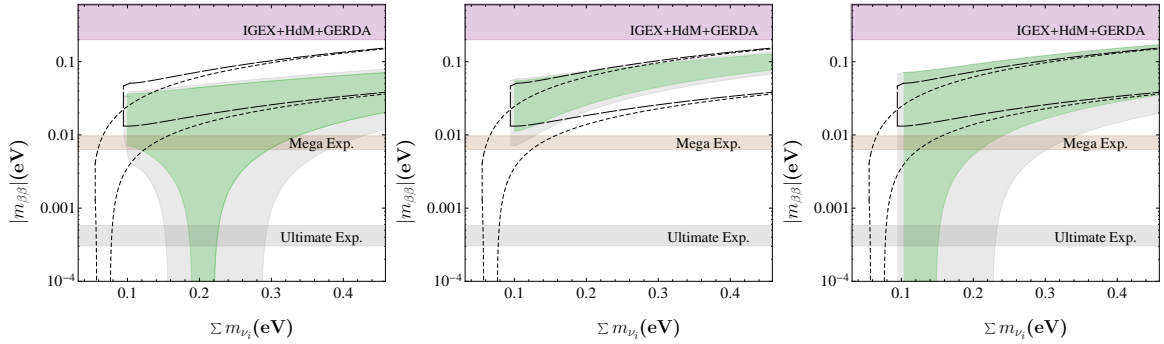


Figure 12. Plots for  $|m_{\beta\beta}|$  vs  $\sum_i m_i$  for the IH case in the presence of one extra sterile neutrino in the case in which respectively, from the left to the right,  $\chi_1$  or  $\chi_2$  or  $\chi_3$  are Dirac fermions. The light (Gray) and darker (Green) shaded areas indicate the allowed range for the  $3\sigma$  and best fit values given in [38].

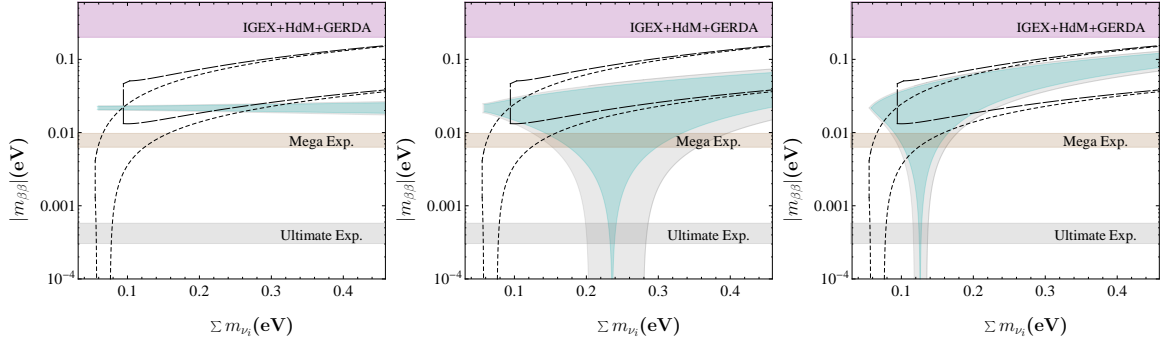


Figure 13. Plots for  $|m_{\beta\beta}|$  vs  $\sum_i m_i$  for the NH case in the presence of one extra sterile neutrino state and in the case in which respectively, from the left to the right,  $(\chi_1, \chi_2)$  or  $(\chi_1, \chi_3)$  or  $(\chi_2, \chi_3)$  are Dirac fermions. The light (Gray) and darker (Blue) shaded areas are given as in Fig. 11.

- [2] DAYA-BAY Collaboration, F. An *et al.*, Phys.Rev.Lett. **108**, 171803 (2012), [1203.1669].
- [3] RENO collaboration, J. Ahn *et al.*, 1204.0626.
- [4] T2K Collaboration, K. Abe *et al.*, Phys.Rev.Lett. **107**, 041801 (2011), [1106.2822].
- [5] Planck Collaboration, P. Ade *et al.*, 1303.5076.
- [6] KATRIN Collaboration, L. Bornschein, eConf **C030626**, FRAP14 (2003), [hep-ex/0309007].
- [7] KATRIN Collaboration, R. H. Robertson, 1307.5486.
- [8] P. Minkowski, Phys.Lett. **B67**, 421 (1977).
- [9] T. Yanagida, Conf.Proc. **C7902131**, 95 (1979).
- [10] M. Gell-Mann, P. Ramond and R. Slansky, Conf.Proc. **C790927**, 315 (1979), [1306.4669].
- [11] J. Schechter and J. W. F. Valle, Phys. Rev. **D22**, 2227 (1980).
- [12] R. N. Mohapatra and G. Senjanovic, Phys.Rev. **D23**, 165 (1981).
- [13] J. W. F. Valle, Phys. Rev. **D27**, 1672 (1983).

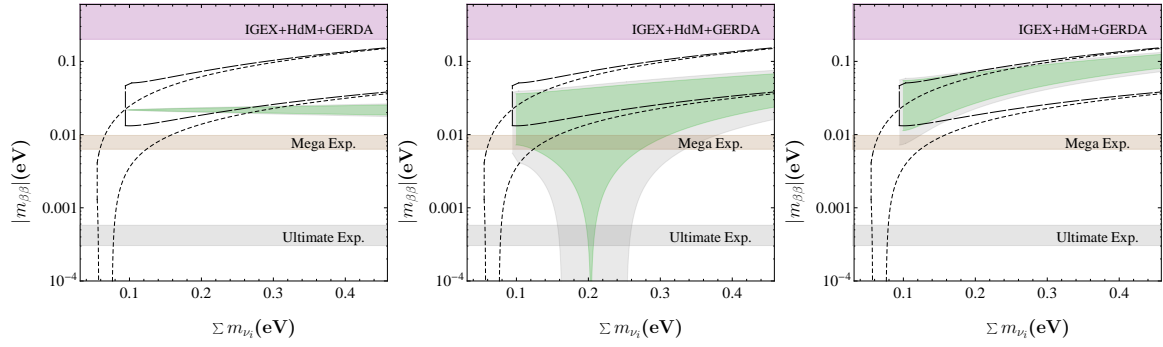


Figure 14. Plots for  $|m_{\beta\beta}|$  vs  $\sum_i m_i$  for the IH case in the presence of one extra sterile neutrino state and in the case in which respectively, from the left to the right,  $(\chi_1, \chi_2)$  or  $(\chi_1, \chi_3)$  or  $(\chi_2, \chi_3)$  are Dirac fermions. The light (Gray) and darker (Green) shaded areas are given as in Fig. 12.

- [14] G. Racah, *Nuovo Cim.* **14**, 322 (1937).
- [15] M. Agostini *et al.*, 1307.4720.
- [16] H. Klapdor-Kleingrothaus, I. Krivosheina, A. Dietz and O. Chkvorets, *Phys.Lett.* **B586**, 198 (2004), [hep-ph/0404088].
- [17] A. Barabash, 1101.4502.
- [18] F. Piquemal, *Nucl.Phys.B, Proc.Suppl.* **235-236**, 273 (2013).
- [19] M. Hirsch, S. Kovalenko and I. Schmidt, *Phys. Lett.* **B642**, 106 (2006), [hep-ph/0608207].
- [20] S. Weinberg, *Phys. Rev.* **D22**, 1694 (1980).
- [21] S. M. Bilenky, S. Pascoli and S. T. Petcov, *Phys.Rev.D* **64**, 053010 (2001), [arXiv:hep-ph/0102265].
- [22] M. Hirsch, *Nucl.Phys.Proc.Suppl.* **221**, 119 (2011), [hep-ph/0609146].
- [23] W. Rodejohann, *Int.J.Mod.Phys.* **E20**, 1833 (2011), [1106.1334].
- [24] Particle Data Group, K. Nakamura and S. Petcov, *Phys.Rev.* **D86**, 010001 (2012).
- [25] KamLAND-Zen Collaboration, A. Gando *et al.*, *Phys.Rev.Lett.* **110**, 062502 (2013), [1211.3863].
- [26] EXO-200 Collaboration, J. Albert *et al.*, 1402.6956.
- [27] S. Dell'Oro, S. Marcocci and F. Vissani, 1404.2616.
- [28] H. Minakata, H. Nunokawa and A. A. Quiroga, 1402.6014.
- [29] S. Dodelson and J. Lykken, 1403.5173.
- [30] EUCLID Collaboration, R. Laureijs *et al.*, 1110.3193.
- [31] D. Meloni, A. Meroni and E. Peinado, *Phys.Rev.* **D89**, 053009 (2014), [1401.3207].
- [32] J. Barry and W. Rodejohann, *Nucl.Phys.* **B842**, 33 (2011), [1007.5217].
- [33] L. Dorame, D. Meloni, S. Morisi, E. Peinado and J. Valle, *Nucl.Phys.* **B861**, 259 (2012), [1111.5614].
- [34] S. F. King, A. Merle and A. J. Stuart, *JHEP* **1312**, 005 (2013), [1307.2901].
- [35] J. Barry, R. N. Mohapatra and W. Rodejohann, *Phys.Rev.* **D83**, 113012 (2011), [1012.1761].
- [36] D. Forero, M. Tortola and J. Valle, 1405.7540.
- [37] M. Gonzalez-Garcia, M. Maltoni, J. Salvado and T. Schwetz, *JHEP* **1212**, 123 (2012), [1209.3023].
- [38] F. Capozzi *et al.*, *Phys.Rev.* **D89**, 093018 (2014), [1312.2878].
- [39] J. Barry, W. Rodejohann and H. Zhang, *JHEP* **1107**, 091 (2011), [1105.3911].
- [40] I. Girardi, A. Meroni and S. Petcov, *JHEP* **1311**, 146 (2013), [1308.5802].
- [41] S. M. Bilenky, S. Pascoli and S. Petcov, *Phys.Rev.* **D64**, 053010 (2001), [hep-ph/0102265].
- [42] L. Wolfenstein, *Nucl.Phys.* **B186**, 147 (1981).
- [43] A. Machado and V. Pleitez, *Phys.Lett.* **B698**, 128 (2011), [1008.4572].
- [44] S. Morisi and E. Peinado, *Phys.Lett.* **B701**, 451 (2011), [1104.4961].
- [45] A. Meroni, S. Petcov and F. Simkovic, *JHEP* **1302**, 025 (2013), [1212.1331].
- [46] LSND Collaboration, A. Aguilar-Arevalo *et al.*, *Phys.Rev.* **D64**, 112007 (2001), [hep-ex/0104049].
- [47] MiniBooNE Collaboration, A. Aguilar-Arevalo *et al.*, *Phys.Rev.Lett.* **110**, 161801 (2013), [1207.4809].
- [48] P. Huber, *Phys.Rev.* **C84**, 024617 (2011), [1106.0687].
- [49] T. Mueller *et al.*, *Phys.Rev.* **C83**, 054615 (2011), [1101.2663].
- [50] F. Kaether, W. Hampel, G. Heusser, J. Kiko and T. Kirsten, *Phys.Lett.* **B685**, 47 (2010), [1001.2731].
- [51] SAGE Collaboration, J. Abdurashitov *et al.*, *Phys.Rev.* **C80**, 015807 (2009), [0901.2200].
- [52] K. Abazajian *et al.*, 1204.5379.
- [53] M. Archidiacono *et al.*, 1404.1794.
- [54] J. Kopp, P. A. N. Machado, M. Maltoni and T. Schwetz, *JHEP* **1305**, 050 (2013), [1303.3011].
- [55] C. Giunti, M. Laveder, Y. Li and H. Long, *Phys.Rev.* **D88**, 073008 (2013), [1308.5288].